Influence of Dynamics on the Changes in Tropical Cloud Radiative Forcing during the 1998 El Niño

Richard P. Allan, A. Slingo, and M. A. Ringer

Hadley Centre for Climate Prediction and Research, Met Office, Bracknell, Berkshire, United Kingdom

ABSTRACT

Satellite measurements of the radiation budget and data from the U.S. National Centers for Environmental Prediction–National Center for Atmospheric Research reanalysis are used to investigate the links between anomalous cloud radiative forcing over the tropical west Pacific warm pool and the tropical dynamics and sea surface temperature (SST) distribution during 1998. The ratio, N, of the shortwave cloud forcing (SWCF) to longwave cloud forcing (LWCF) ($N = -$SWCF/LWCF) is used to infer information on cloud altitude. A higher than average N during 1998 appears to be related to two separate phenomena. First, dynamic regime-dependent changes explain high values of N (associated with low cloud altitude) for small magnitudes of SWCF and LWCF (low cloud fraction), which reflect the unusual occurrence of mean subsiding motion over the tropical west Pacific during 1998, associated with the anomalous SST distribution. Second, Tropics-wide long-term changes in the spatial-mean cloud forcing, independent of dynamic regime, explain the higher values of N during both 1998 and in 1994/95. The changes in dynamic regime and their anomalous structure in 1998 are well simulated by version HadAM3 of the Hadley Centre climate model, forced by the observed SSTs. However, the LWCF and SWCF are poorly simulated, as are the interannual changes in N. It is argued that improved representation of LWCF and SWCF and their dependence on dynamical forcing are required before the cloud feedbacks simulated by climate models can be trusted.

1. Introduction

The profound impact of clouds on the earth's radiative balance and hence their potential contribution to climate feedbacks is well documented [e.g., Ramanathan et al. 1989; Slingo 1990; Houghton et al. 2001]. One of the most important perturbations to tropical cloud cover on interannual timescales is provided by El Niño. While the relevance to the cloud feedbacks that may occur on longer timescales during global warming is unclear, the cloud radiation changes on shorter timescales present an opportunity to improve our understanding of the underlying physical processes operating within the climate system.

Cess et al. (2001) analyzed broadband radiation budget data for 1985–90 from the Earth Radiation Budget Experiment (ERBE; Harrison et al. 1990) and for 1998 from the Clouds and the Earth's Radiant Energy System instrument (CERES; Wielicki et al. 1996) on the Tropical Rainfall Measuring Mission satellite. Their analysis was in terms of the longwave (LW), shortwave (SW), and net (NET) cloud radiative forcing (CF) diagnostic and the ratio, $N = -$SWCF/LWCF. For definitions and

Corresponding author address: Dr. Richard P. Allan, Hadley Centre for Climate Prediction and Research, Met Office, London Road, Bracknell, Berkshire RG12 2SY, United Kingdom.
E-mail: richard.allan@metoffice.com

background, see Cess et al. (2001). As noted by Kiehl and Ramanathan (1990), over regions of deep tropical convection the values of LW and SW CF are large and similar in magnitude although they have opposing signs, so that NET CF is approximately zero and $N \sim 1$. Kiehl (1994) argued that this near cancellation is caused by deep, optically thick clouds with tops located near the tropical tropopause. This conclusion has been challenged by Hartmann et al. (2001), who argue that the cancelation is explained by the arrangement of an ensemble of cloud types associated with deep convection, which exert both positive and negative influences on the top of atmosphere radiation budget.

Cess et al. (2001) noted that the near cancellation between the SW and LW CF over the tropical west Pacific warm pool was evident during the ERBE period but not during the CERES observations of the 1998 El Niño, when SWCF dominated over LWCF. They interpreted this result as being due to lower average cloud-top heights during this event. Here, we show that this result is partly due to changes in the prevailing dynamical regime during the 1998 El Niño in this region and partly to longer period changes that are as yet unexplained. We also examine the ability of the Hadley Centre climate model to reproduce these changes, assessing whether an atmospheric model forced with observed sea surface temperatures (SSTs) demonstrates skill in simulating tropical CF and its variability.

TABLE 1. Jan–Aug mean cloud radiative forcing quantities from satellite observations and 500-hPa vertical velocity from the NCEP–NCAR reanalysis for the tropical Pacific warm pool region (5°S–5°N, 145°–165°E).

Year	$\overline{\text{SWCF}}$ (W m^{-2})	$\overline{\text{LWCF}}$ (W m^{-2})	$\overline{\text{NET CF}}$ (W m^{-2})	$\overline{N}$	$\overline{\omega}$ (Pa s^{-1})
1985	−67	62	−5	1.08	−0.044
1986	−74	68	−5	1.08	−0.042
1987	−70	61	−9	1.14	−0.035
1988	−64	58	−5	1.09	−0.033
1999	−66	61	−5	1.08	−0.032
1994/95	−73	61	−12	1.20	−0.040
1998	−53	41	−12	1.29	−0.019

2. Results

We use monthly mean top of atmosphere radiation budget data from CERES (version 2) for 1998; the *Earth Radiation Budget Satellite* (*ERBS*), which formed the main component of the ERBE mission) for the period 1985–89; and from the first Scanner for Radiation Budget instrument (ScaRaB; Kandel et al. 1998), which operated on the *METEOR-3/7* satellite during 1994 and 1995. Vertical velocities and surface temperatures were taken from the National Centers for Environmental Prediction–National Center for Atmospheric Research (NCEP–NCAR) 40-yr reanalysis (Kalnay et al. 1996), hereafter referred to as NCEP. For consistency with Cess et al. (2001), the Pacific warm pool region was defined as 5°S–5°N and 140–165°E and January–August monthly mean data were considered. For the 1994/95 period, ScaRaB data for January and February 1995 and March–August 1994 were used; April was not considered in this period due to missing data. In the present study, quantities with an overbar have been computed from space–time means of their component terms. Thus, $\overline{\text{LWCF}}$ is calculated as the difference between the space–time mean of clear-sky and all-sky outgoing longwave radiation (OLR). Where no overbars are included, the quantity represents gridpoint monthly mean values.

Table 1 shows the Pacific warm pool $\overline{\text{CF}}$ and $\overline{N}$ for *ERBS* (1985–89), ScaRaB (1994/95), and CERES (1998). Here $\overline{N}$ was calculated using the 8-month spatial means of LW and SW CF. Also shown in Table 1 is the NCEP 500-hPa vertical velocity $\overline{\omega}$ (Pa s^{-1}). Observed values of LW and SW CF in Table 1 are significantly lower in 1998 than given by Cess et al. (2001), who used a preliminary version of the CERES data. Nevertheless, comparing scanning radiometer data with ERBS nonscanner data during overlap periods suggests that tropical mean OLR anomalies are consistent to within about 1 W m^{-2} (Wielicki et al. 2002). This improves confidence in the comparisons of such scanning radiometer products in the present study.

Table 1 shows anomalously low LW and SW CF in 1998 compared to other years, as identified by Cess et al. (2001). Despite the stability of the mean SST, varying by only about ±0.2 K from year to year, the NCEP 500-

hPa vertical velocity in 1998 is less negative than in the other years. This offers a clue as to the reason for the unusual CF in 1998. However, while N is indeed greater in 1998 than 1985–89 (indicating reduced cloud altitude for 1998), the corresponding value for 1994/95 also appears significantly higher than the 1985–89 period. Thus, contrary to the findings of Cess et al. (2001), the anomalous CF in the tropical west Pacific does not appear to be solely related to the strength of the 1998 El Niño.

Scatterplots of observed monthly mean, gridpoint values of N (calculated from monthly, gridpoint LW and SW CF) with corresponding −SWCF are presented in Fig. 1. Diagonal lines follow contours of LWCF. The line, $N = 1$, is also marked, highlighting where NET CF is zero. The method is similar to that shown in Fig. 5 of Cess et al. (2001), but clarifies the magnitudes of LWCF and SWCF and also does not exhibit the problematic convergence of points at $N = 1$, NET CF = 0. For a given value of SWCF, increasing N generally indicates lower altitude cloud tops while larger magnitudes of SWCF indicate greater optical depth or cloud fraction.

The observed N–SWCF scatter in Figs. 1a–e all show a general increase in N with |SWCF|, although 1987 and 1994/95 show slightly greater scatter. The distribution is symptomatic of high-altitude cloud of variable thickness, as discussed by Cess et al. (2001), with optical depth increasing with the magnitude of SWCF. While this relationship is also present to some degree in 1998 (Fig. 1d), there are also higher values of N for |SWCF| < 40 W m^{-2}, indicative of lower altitude cloud. Because these points display small LWCF (<20 W m^{-2}), as well as a low magnitude of SWCF, these grid points likely contain relatively small amounts of cloud cover.

The unusual influence of low-altitude cloud tops and low CF on the top of atmosphere radiation budget during 1998 appears consistent with the anomalously weak mean ascending motion diagnosed from NCEP vertical velocity (Table 1). For example, one might expect higher values of N in regions of large-scale descent because low-altitude clouds will predominate over deeper, higher altitude clouds. Indeed, the gridpoint values of N exhibit a strong dependence on vertical velocity with low values of N coinciding with convective regimes and higher N for suppressed regimes (Cess et al. 2001). It is thus expected that the changes in convective regime hinted at in Table 1 could explain some of the changes in the nature of the N–SWCF relationship. However, reduced vertical motion in the tropical west Pacific is unlikely to explain the high value of $\overline{N}$ apparent during 1994/95, where the distribution of CF and the vertical velocities appear consistent with the 1985–89 period (Table 1 and Fig. 1). To remove the effects of changes in dynamical regime on the CF, the analysis is now restricted to regions of strongest mean ascent, normally experienced in the tropical warm pool region.
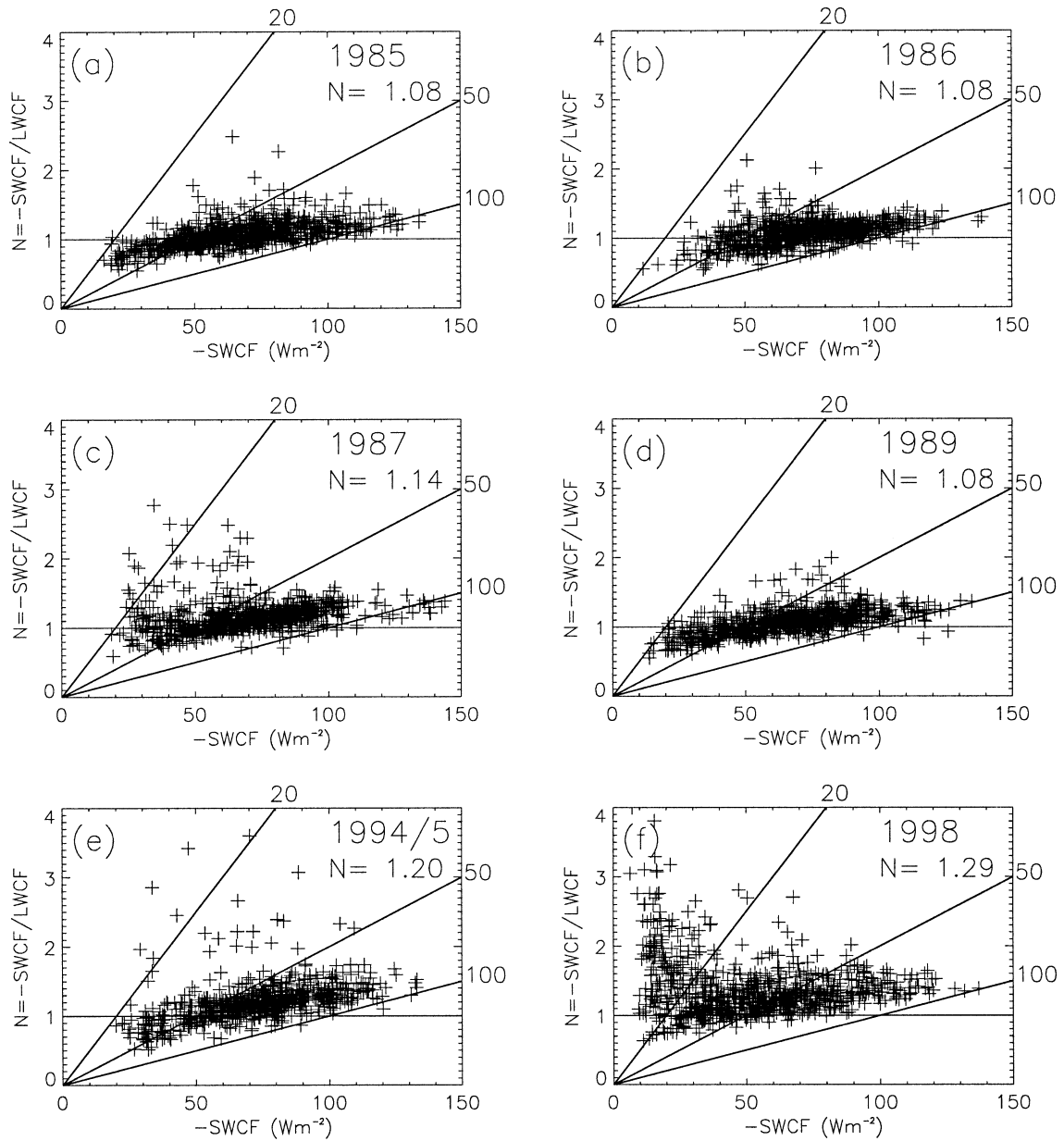
FIG. 1. Satellite observations of gridpoint monthly mean N as a function of SWCF for Jan–Aug (1985, 1986, 1987, 1989, 1994/95, 1998) in the tropical west Pacific warm pool (5°S–5°N, 140°–165°E). Diagonal lines follow contours of LWCF for 20, 50, and 100 W m^{-2}. Here $\overline{N}$ is displayed for each year.

Figure 2 shows data from the NCEP reanalysis combined with the satellite CF observations over the entire tropical Pacific (20°S–20°N and 100°–270°E) for the time periods used in Figs. 1c–f. The box shows the tropical warm pool region considered previously. On the left, NCEP surface temperatures (darker shading indicating colder temperatures) are displayed with overlaid contours of NCEP 500-hPa vertical velocity (solid lines denote mean ascent while dashed lines indicate mean descent or neutral conditions). The observed monthly mean gridpoint N–SWCF relationships for the corresponding years are plotted on the right, but only

for grid points containing strong convection, defined here by $\omega < -0.06$ Pa s^{-1}.

It is apparent from Fig. 2 that the regions of strongest mean ascent generally coincide with the warmest SSTs. Further, it is striking that the anomalous observed N–SWCF scatter for the tropical warm pool in 1998 (Fig. 1d) is not present when sampling only regions of strong ascent over the tropical Pacific (Fig. 2h). However, the anomalously high values of $\overline{N}$ in 1998 and 1994/95 over the tropical west Pacific warm pool remain evident when considering only regions where $\omega < -0.06$ Pa s^{-1} over the entire tropical Pacific. This result is also independent
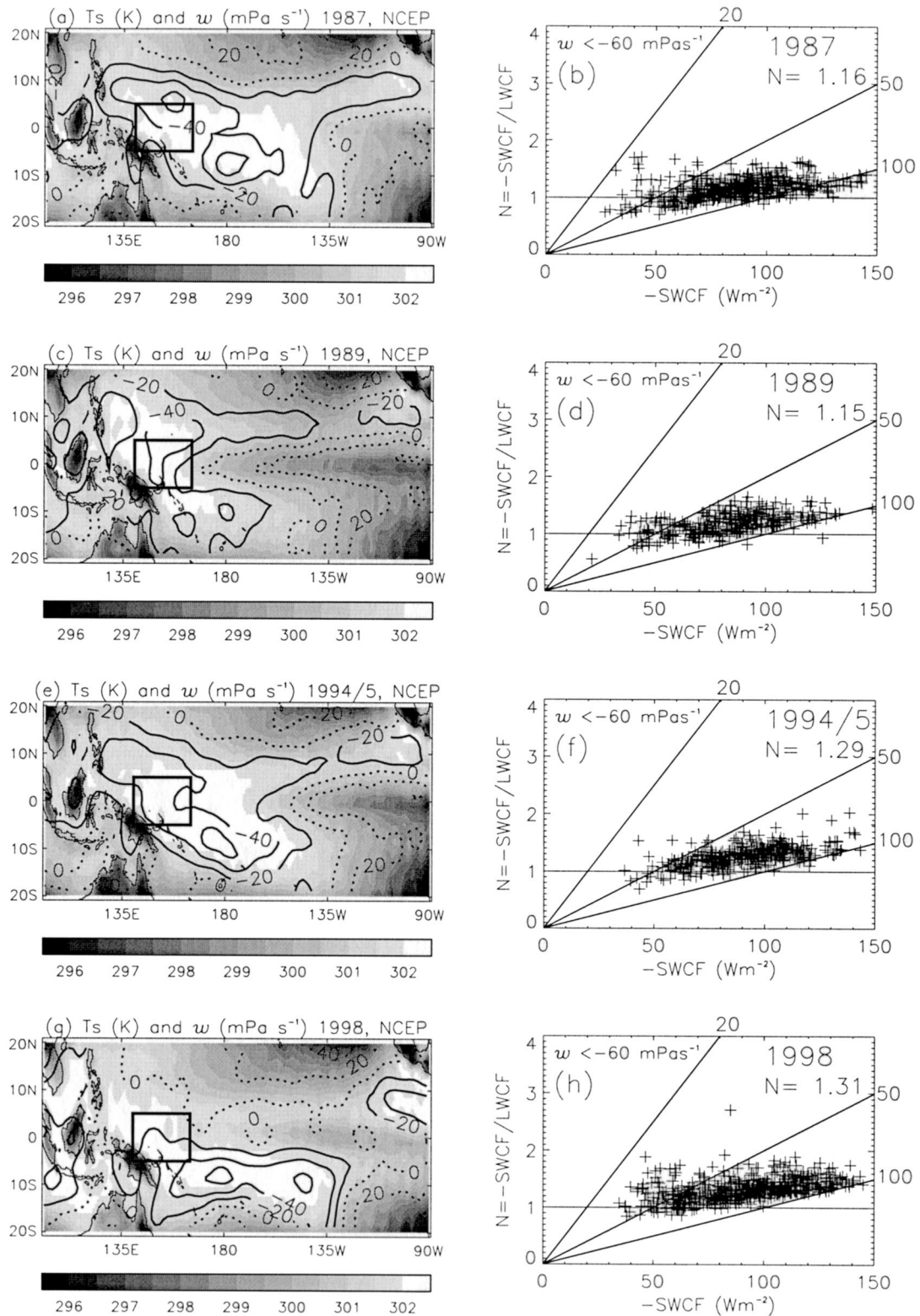
FIG. 2. Tropical Pacific surface temperature T_s (K; grayscale), with overlaid 500-hPa vertical velocity, ω (mPa s^{-1}), from the NCEP reanalysis using Jan–Aug averages for (a) 1987, (c) 1989, (e) 1994/95, and (g) 1998. The tropical west Pacific warm pool region (5°S–5°N, 140°–165°E) is marked. (b), (d), (f), (h) Scatterplots for observed monthly mean gridpoint values of N vs SWCF (W m^{-2}) for NCEP $\omega < -60$ mPa s^{-1} are shown and $\overline{N}$ displayed for the corresponding years.

of the tropical region chosen and the dynamical regime analyzed, provided that the mean ω for each year does not change significantly. When the analysis is repeated for different dynamical regimes, the N–SWCF distribution alters as the ω range is changed but affects a similar distribution for each year when the mean ω remains constant.

From this analysis of the satellite observations of CF and NCEP vertical velocity and SST, it is apparent that the strong El Niño of 1998 caused a large perturbation to the atmospheric circulation, resulting in the anomalous CF identified by Cess et al. (2001). The unusual infiltration of descending air into the tropical west Pacific warm pool appears to explain the occurrence of low magnitude values of CF with a high ratio of −SWCF/LWCF, symptomatic of small cloud fraction and low-altitude cloud tops. However, reductions in the area-mean effective cloud altitude, as diagnosed from $\overline{N}$, cannot be explained solely by these changes for two reasons. First, the 1994/95 period, which shows no significant differences in dynamic regime for the west Pacific warm pool to the 1985–89 period, also displays a value of $\overline{N}$ significantly greater than 1985–89. Second, when considering only strongly convective dynamic regimes over the tropical Pacific, thus removing the changes in cloud related to variation of mean vertical motion, the anomalously high values of $\overline{N}$ for 1994/95 and 1998 remain.

3. Model simulations

Having established significant variability in the observed CF fields in the Tropics, related to changes in dynamic regime and to longer-term unexplained variations, we now consider the degree to which the observed cloud radiative effects can be simulated by a climate model. This is particularly important given the sensitivity of current climate predictions to the formulation of convective processes and their influence on cloud feedback (Houghton et al. 2001). We employ the 19 vertical level, $2.5°$ lat $\times$ $3.75°$ lon horizontal resolution atmosphere-only version of the Hadley Centre climate model (HadAM3). The model employs a mass flux scheme for moist and dry convection including downdrafts and is described in detail by Pope et al. (2000). To provide a consistent comparison with the observed variations in the radiation budget, simulations forced by the observed SSTs and sea ice fields of the Global Sea Ice and SST dataset (GISST; Rayner et al. 1998) are used. For experimental details, see Sexton et al. (2001).

The analysis presented in Fig. 2 is reproduced using output from HadAM3 in Fig. 3. This methodology ensures that local differences between observed and simulated dynamical fields do not influence the comparisons of CF, thereby allowing a consistent comparison of the cloud radiative effects for a given dynamic regime. The simulated vertical motion fields and their relation to the

SST distribution show excellent agreement with the NCEP values displayed in Fig. 2. The incursion of mean subsidence into the tropical west Pacific region in 1998 is captured by the model, although it is slightly more pronounced than in the NCEP data. This suggests that the movement of dynamic regimes in association with changes in the SST distribution, important for the spatial redistribution of cloud systems, is well simulated. Indeed, there is an increased occurrence of gridpoints in this region containing low magnitudes of LWCF and SWCF during 1998 compared to other years.

The simulated N–SWCF distributions for strongly convective regions ($\omega < -0.06$ Pa s^{-1}) is similar for each year considered. However, there are important differences between the observations and the model simulations with regard to the SW and LW CF magnitudes. For example, for the tropical west Pacific warm pool region, January–August mean CF is underestimated by between 6% and 23% for the SW and 13%–42% for the LW (not shown). The underestimation of CF is common to many models (Houghton et al. 2001) and is consistent with previous evaluations of HadAM3 for the tropical warm pool Pacific region (Pope et al. 2000). Some of these differences are related to underestimated cloud fraction. However, for convective regimes, the model overestimates $\overline{N}$, suggesting that the effective cloud altitude for HadAM3 is too low. While the observed $\overline{N}$ is close to unity, indicating near cancellation of the SW and LW CRF components, the simulated value is somewhat higher, indicating that the cloud reflectivity is unrealistically dominating over the greenhouse trapping in HadAM3. Further, the observed tendency for values of $\overline{N}$ to be higher during 1994/95 and 1998 relative to 1985–89 is not evident in the simulations.

A note of caution should be made regarding the comparisons of CF and N between the model and observations. Satellite clear-sky fluxes are sampled only where the scene is determined to be free of cloud. Model clear-sky fluxes, however, are calculated for all regions in an additional diagnostic calculation by setting the cloud fraction to zero. Therefore, the model will effectively sample the generally humid cloudy regions not included in the observations. The higher effective humidity used in the model computations will act to produce a low bias in the clear-sky outgoing LW and SW radiation relative to the observations, due to additional water vapor absorption, thus causing the model SWCF to be biased high and the LWCF to be biased low (e.g., Cess and Potter 1987). This inconsistent sampling of clear-sky fluxes between the model and the observations is expected to cause simulated values of $\overline{N}$ to be greater than observed values. Despite this, the model-observed CF differences are significantly greater than the expected biases due to the effect of inconsistent clear-sky sampling. Also, these systematic biases cannot explain the smaller simulated variability of $\overline{\text{CF}}$ and $\overline{N}$ compared to the satellite observations.
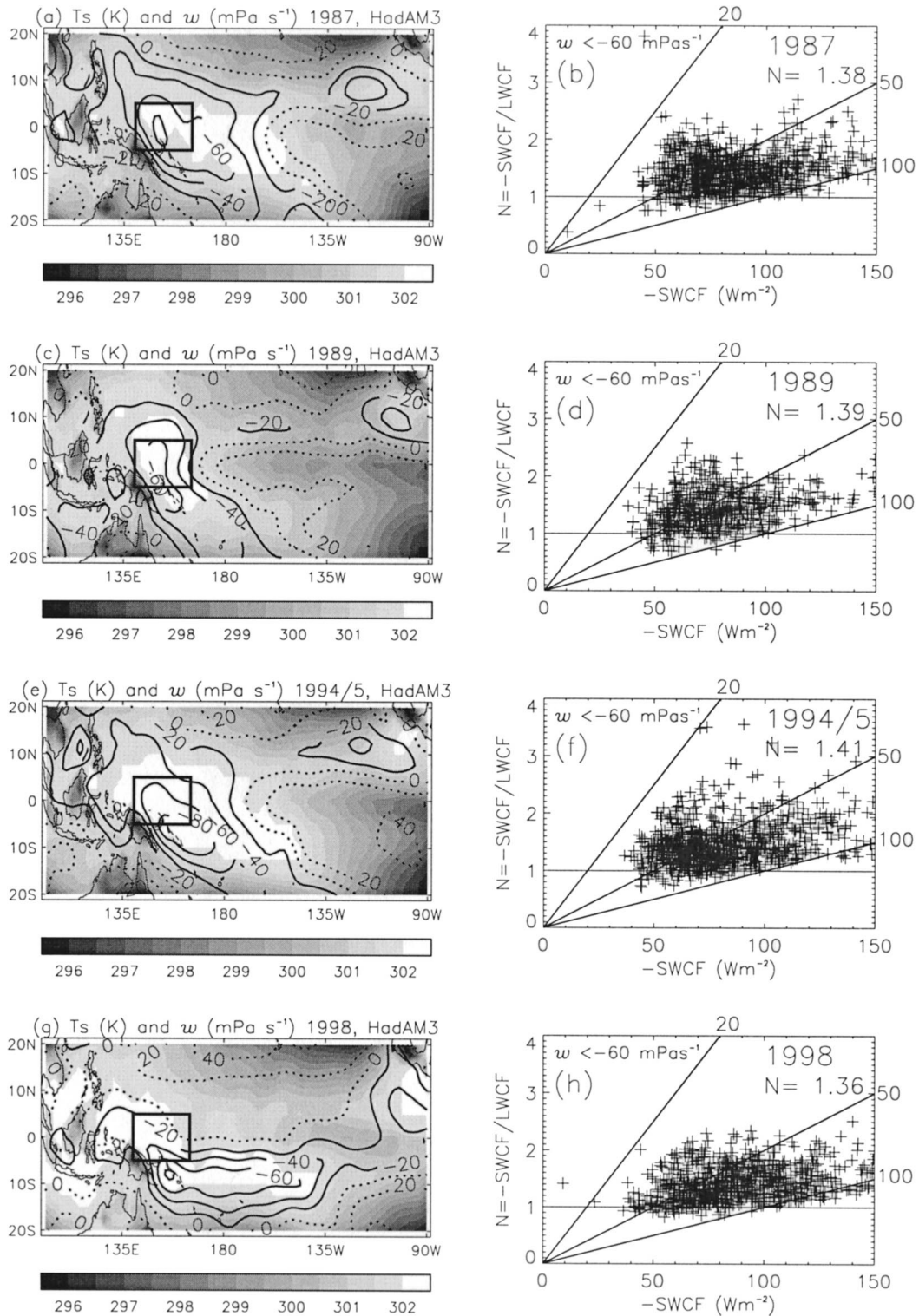
FIG. 3. Tropical Pacific surface temperature, T_s (K; grayscale), from HadAM3 with overlaid 500-hPa vertical velocity, ω (mPa s^{-1}), using Jan–Aug averages for (a) 1987, (c) 1989, (e) 1994/95, and (g) 1998. The tropical west Pacific warm pool region bounded by 5°S, 5°N, 140°E, and 165°E is marked. (b), (d), (f), (h) Scatterplots for simulated monthly mean gridpoint values of N vs SWCF (W m^{-2}) where $\omega < -60$ mPa s^{-1} are shown and $\bar{N}$ displayed for the corresponding years.

TABLE 2. Jan–Aug tropical mean (30°S–30°N) cloud radiative forcing quantities inferred from satellite observations and simulated by HadAM3. Model values (in parentheses) represent five-member ensemble means with error bars denoting the 2 × interensemble std dev ($\pm2\sigma$).

Year	$\overline{\text{SWCF}}$ (W m^{-2})	$\overline{\text{LWCF}}$ (W m^{-2})	$\overline{\text{NET CF}}$ (W m^{-2})	$\overline{N}$
1985	−44.4 (−45.9 ± 0.6)	32.5 (22.5 ± 0.2)	−11.9 (−23.5 ± 0.4)	1.37 (2.05 ± 0.02)
1986	−43.9 (−45.8 ± 0.8)	32.2 (22.5 ± 0.2)	−11.6 (−23.4 ± 0.8)	1.36 (2.04 ± 0.03)
1987	−43.0 (−46.0 ± 0.6)	31.6 (22.6 ± 0.3)	−11.4 (−23.4 ± 0.6)	1.36 (2.04 ± 0.03)
1988	−44.1 (−46.5 ± 0.5)	31.9 (22.6 ± 0.5)	−12.2 (−24.0 ± 0.4)	1.38 (2.06 ± 0.03)
1989	−43.6 (−45.3 ± 0.4)	32.1 (22.6 ± 0.4)	−11.5 (−22.7 ± 0.4)	1.36 (2.01 ± 0.02)
1994/95	−45.2 (−47.1 ± 0.5)	28.6 (22.5 ± 0.1)	−16.6 (−24.6 ± 0.5)	1.58 (2.09 ± 0.03)
1998	−43.7 (−45.9 ± 0.5)	28.4 (22.4 ± 0.4)	−15.3 (−23.5 ± 0.5)	1.54 (2.05 ± 0.04)

4. Tropical means

Table 2 presents a summary of the observed and simulated changes in the radiation budget, averaged over the entire Tropics (30°S–30°N). The observed large-scale change in $\overline{N}$ noted earlier is still evident and appears to be related primarily to a decrease in $\overline{\text{LWCF}}$ (note the values in the last two lines of Table 2, compared with those above). Again, the anomalous values of $\overline{N}$ do not apply exclusively to 1998; observed values of $\overline{N}$ below 1.4 for the 1985–89 period increase to above 1.5 during 1994/95 and 1998. While the observed SWCF shows no significant change between each period, there is a reduction of LWCF from about 32 W m^{-2} in the 1985–89 period to below 29 W m^{-2} afterward. This change appears to be significant, given that tropical mean OLR anomalies are consistent to within 1 W m^{-2} (Wielicki et al. 2002). The model simulations (values displayed in parentheses in Table 2) do not capture the change in LWCF, with values remaining remarkably constant at about 22 W m^{-2}, significantly lower than the observations. In addition, the high value of $\overline{N}$ simulated by the model shows no significant change in time.

This suggests that the results presented in Cess et al. (2001) are related to two separate phenomena. The anomalous N–SWCF distribution during 1998 for the Pacific warm pool region can be explained in terms of the anomalous band of high SSTs situated around 10°S from 140° to 220°E and its associated regions of strongest ascent, conditions normally predominant over the tropical warm pool. These changes are well simulated when observed SSTs are used to force the climate model. It is clear from Figs. 2 and 3 that an area of mean descent, usually restricted to the north of the 10°N lat band, extended south into the Pacific warm pool, introducing a dynamic regime unusual to the region. This regime generally contains lower altitude clouds of characteristically high values of N, thus explaining the different N–SWCF scatter in 1998. However, the climate model poorly represents the CF and the diagnosed effective cloud altitude. The temporal changes in $\overline{N}$ over the tropical warm pool and the entire Tropics are also not simulated by the climate model and further cannot be explained solely in terms of changes in mean ascent for the regions considered. Also, they do not apply exclusively to 1998 and therefore cannot solely be due to the exceptional strength of the 1997/98 El Niño event as argued in Cess et al. (2001). They appear instead to be a manifestation of longer period changes over the entire Tropics (Wielicki et al. 2002), the cause of which is currently under investigation.

5. Summary

Anomalous cloud radiative forcing in the tropical warm pool region during the El Niño event of 1998 was diagnosed by Cess et al. (2001) using the ratio, N, of shortwave and longwave CF and its relationship with net CF. Relative to the 1985–89 period, a greater scatter of N and net CF and an increased value of $\overline{N}$ was apparent during 1998. This was explained by Cess et al. (2001) in terms of a reduced occurrence of high-altitude clouds (ranging from deep convective to thin cirrus) and the increased occurrence of midlevel clouds.

Using NCEP reanalysis vertical velocity data in combination with the observed radiation budget data, it is shown in the present study that the anomalous CF in 1998 relates to two separate phenomena. First, a higher than normal occurrence of grid points exhibiting low-magnitude LW and SW CF (suggesting reduced cloud fraction) and anomalously high N (indicating reduced cloud altitude) operated during 1998. This is related to the unusual encroachment of subsiding motion into the tropical warm pool region and is linked to the anomalous SST distribution of 1998. Large-scale subsiding motion favors lower-altitude cloud tops and smaller cloud fraction compared to convective regimes. However, these dynamical related changes in CF do not explain the high $\overline{N}$ experienced during the 1994/95 ScaRaB period, when the tropical west Pacific warm pool was not affected by unusual mean vertical motion. Further, the high values of $\overline{N}$ in 1994/95 and 1998 remain when only gridpoints containing strong ascent (defined as $\omega < -0.06$ Pa s^{-1}) are sampled, thereby removing the dependence on changes in dynamic regime. An additional explanation for the anomalous CF in 1994/95 and 1998, which appears to apply to the entire Tropics, is therefore required. Wielicki et al. (2002) show that these changes are not

due to instrumental artefacts but are associated with decadal variations in tropical cloudiness and are not directly associated with El Niño.

A version of the Hadley Centre climate model (HadAM3) forced by observed SSTs, covering the period of the satellite data, displays unrealistic CF, indicating deficiencies in the simulated tropical cloud radiative effect. Nevertheless, despite the shortcomings of HadAM3, the model successfully simulates the changes in the spatial distribution of the vertical motion fields. This suggests that changes in cloud regimes linked to the movement of rising and descending branches of the large-scale circulation, that are intrinsically linked to the SST distribution, can be simulated with reasonable accuracy. However, the inaccurate simulations of the distribution and properties of cloud mean that the magnitude changes in cloud radiative effect, related to local changes in dynamic regime, may still be poorly simulated. The climate model fails to simulate the apparent longer-term variation in effective cloud radiative altitude, diagnosed from $\overline{N}$. Given the uncertainty in cloud feedbacks and their importance with respect to future climate predictions, the observed cloud forcing and its variability provide an important means of testing and improving climate models. Without such validation, the accurate simulation of cloud feedbacks remains in question.

REFERENCES

Cess, R. D., and G. L. Potter, 1987: Exploratory studies of cloud radiative forcing with a general circulation model. *Tellus,* **39,** 460–473.

——, M. Zhang, B. A. Wielicki, D. F. Young, X. Zhou, and Y. Nikitenko, 2001: The influence of the 1998 El Niño upon cloud radiative forcing over the Pacific warm pool. *J. Climate,* **14,** 2129–2137.

Harrison, E. F., P. Minnis, B. R. Barkstrom, V. Ramanathan, R. Cess, and G. G. Gibson, 1990: Seasonal variation of cloud radiative forcing derived from the Earth Radiation Budget Experiment. *J. Geophys. Res.,* **95,** 18 687–18 703.

Hartmann, D. L., L. A. Moy, and Q. Fu, 2001: Tropical convection and the energy balance at the top of the atmosphere. *J. Climate,* **14,** 4495–4511.

Houghton, J. T., Y. Ding, D. J. Griggs, M. Noguer, P. J. van der Linden, X. Dai, K. Maskell, and C. A. Johnson, Eds., 2001: *Climate Change 2001: The Scientific Basis.* Cambridge University Press, 881 pp.

Kalnay, E., and Coauthors, 1996: The NCEP/NCAR 40-Year Reanalysis Project. *Bull. Amer. Meteor. Soc.,* **77,** 437–471.

Kandel, R., and Coauthors, 1998: The ScaRaB radiation budget dataset. *Bull. Amer. Meteor. Soc.,* **79,** 765–783.

Kiehl, J. T., 1994: On the observed near cancellation between longwave and shortwave cloud forcing in tropical regions. *J. Climate,* **7,** 559–565.

——, and V. Ramanathan, 1990: Comparison of cloud forcing derived from the earthradiation budget experiment with that simulated by the NCAR community climate model. *J. Geophys. Res.,* **95,** 11 679–11 698.

Pope, V. D., M. L. Gallani, P. R. Rowntree, and R. A. Stratton, 2000: The impact of new physical parameterizations in the Hadley Centre climate model—HadAM3. *Climate Dyn.,* **16,** 123–146.

Ramanathan, V., R. D. Cess, E. F. Harrison, P. Minnis, B. R. Barkstrom, E. Ahmad, and D. Hartmann, 1989: Cloud-radiative forcing and climate: Results from the Earth Radiation Budget Experiment. *Science,* **243,** 57–63.

Rayner, N. A., E. B. Horton, D. E. Parker, and C. K. Folland, 1998: Versions 2.3b and 3.0 of the Global Sea Ice and Sea Surface Temperature (GISST) data set. Hadley Centre Internal Note 85, 98 pp. [Available from Hadley Centre for Climate Prediction and Research, Met Office, London Road, Bracknell, Berkshire RG12 2SY, United Kingdom.]

Sexton, D. M. H., D. P. Rowell, C. K. Folland, and D. J. Karoly, 2001: Detection of anthropogenic climate change using an atmospheric GCM. *Climate Dyn.,* **17,** 669–685.

Slingo, A., 1990: Sensitivity of the earth's radiation budget to changes in low clouds. *Nature,* **343,** 49–51.

Wielicki, B. A., B. R. Barkstrom, E. F. Harrison, R. B. Lee, G. L. Smith, and J. E. Cooper, 1996: Clouds and the Earth's Radiant Energy System (CERES): An earth observing system experiment. *Bull. Amer. Meteor. Soc.,* **77,** 853–868.

——, and Coauthors, 2002: Evidence for large decadal variability in the tropical mean radiative energy budget. *Science,* **295,** 841–844.